2014

Evaluation And Characterization Of The Biomechanical Properties Of Tissue Engineered Vascular Grafts Implanted In The Arterial Circulation

Brooks Van Udelsman
Yale School of Medicine

Evaluation and characterization of the biomechanical properties of tissue engineered vascular grafts implanted in the arterial circulation.

A Thesis Submitted to the
Yale University School of Medicine
in Partial Fulfillment of the Requirements for the
Joint Degree of Doctor of Medicine and Master of Health Science

by

Brooks Van Udelsman

2014

Abstract:

We used a murine model to assess *in vivo* the evolving biomechanical properties of tissue engineered vascular grafts (TEVGs) implanted in the arterial circulation. The initial polymeric tubular scaffold was fabricated from (poly)lactic acid (PLA) and coated with a 50:50 copolymer of (poly)caprolactone and (poly)lactic acid (P[PC/LA]). Following seeding with syngeneic bone marrow derived mononuclear cells, the TEVGs (n=50) were implanted as aortic interposition grafts in wild-type mice and monitored serially using ultrasound. A custom biaxial mechanical testing device was used to quantify *in vitro* the circumferential and axial mechanical properties of grafts explanted at 3 or 7 months. At both times, the TEVGs were biaxially stiffer than native tissue. We treated the TEVGs with either elastase or collagenase to delineate individual contributions of these structural proteins to the overall properties. Elastin conferred an insignificant contribution whereas collagen contributed significantly to TEVG stiffness. The mechanical properties were compared with the underlying microstructure, which was inferred from traditional histology and immunohistochemistry. Analysis revealed smooth muscle cell layers, appropriate collagen deposition, and increasing elastin production. In addition, significant amounts of residual scaffold were present at both 3 and 7 months, which likely contributed to the high stiffness seen in mechanical testing. These results suggest that PLA may have inadequate degradation *in vivo*, which impairs cell-mediated development of vascular neotissue having properties closer to native arteries. Assessing contributions of individual components, such as elastin and

collagen, to the developing neovessel promises to guide computational modeling that may help to optimize the design of the TEVG.

ACKNOWLEDGEMENTS:

This thesis was done under the supervision of Dr. Christopher K. Breuer, M.D., of the Department of Surgery, Division of Pediatric Surgery, and Dr. Jay D. Humphrey of the School of Engineering and Applied Science, Department of Biomedical Engineering. I am very grateful for their guidance, support, and mentorship during my medical school training. Additionally, I am indebted to my thesis advisors, Drs. Alan Dardik and Laura Niklason, for their expert advice on this project.

I would also like to extend my warmest gratitude to the many individuals who helped with this project, including Ramak Khosravi, Ethan Dean, Kristin Miller, Jacopo Ferruzzi, Matthew Bersi, Mark Maxfield, Kevin Rocco, Angela Huang, and Tai Yi.

This project would not have been accomplished without the support and encouragement of the Office of Student Research. Funding was obtained through the Howard Hughes Medical Fellows program and I am especially grateful to all the effort and help provided by Melanie Daub. Additional funding came from the NIH: R01-HL098228 (C. Breuer) and 5T32-HL098069 (A. Sinusas).

Finally, this thesis is dedicated to my grandparents Paul and Sandra Goldner for their unwavering love and support as well as my late great uncle Stanley Warmflash for his commitment to faith and sense of humor.

Table of Contents:

Introduction:

Clinical Problem- Cardiovascular Disease:

Cardiovascular disease (CVD) is the number one killer in the United States, accounting for 1 of every 3 deaths.[1] In the pediatric population, congenital heart defects (CHD) are the most common congenital malformation in newborns, found in 1% of all live births.[1] Similarly, the prevalence of peripheral arterial disease (PAD) in the United States is estimated to be 4.3%, which corresponds to roughly 5 million individuals.[2]

While CVD, CHD, and PAD represent diverse pathology and structural defects, they are linked by resulting ischemia caused by obstruction or misdirection of blood flow. In the adult population, ischemia in the coronary circulation can trigger myocardial infarction (MI) whereas ischemia in the peripheral circulation can cause claudication and contribute gangrenous necrosis. In the pediatric population, the severity CHD affecting the heart and great vessels is based on the degree of cyanosis that is often caused by the mixing of deoxygenated blood intended for the pulmonary circulation with oxygenated blood intended for the systemic circulation. In addition, rare congenital defects resulting in stenosis of the great vessels such as midaortic syndrome (MOS) are associated with significant morbidity and mortality due to severe intractable hypertension and impaired blood flow to the kidneys and lower extremities.[3,4]

Synthetic Vascular Grafts:

The clinical link between CVD, CHD, and PAD is the need for revascularization procedures. Currently, native vessels represent the gold standard for revascularization. Even so, commonly used graft vessels such as the great saphenous vein have a 39% stenosis rate secondary to intimal hyperplasia by 10 years after implant.[5] Moreover, such autologous grafts are not always an option due to limited availability and concurrent disease. Synthetic alternatives such as (poly)tetrafluoroethylene (Gortex®, W.L. Gore & Associates, Newark, DE) and (poly)ethylene terephthalate (Dacron®, Dupont, Wilmington, DE) have several limitations, including innate thrombogencity, risk of infection, and aneurysm formation.[6] In the pediatric population, synthetic grafts are further limited by their lack of growth potential.[7]

Notable examples of the limitations of synthetic grafts in the pediatric population include single ventricle physiology CHD and midaortic syndrome. The standard of care for correction of single ventricle physiology CHD is a staged surgical reconstructive operation known as the Fontan procedure. Classically, a Glenn shunt (a superior vena cava to right pulmonary artery anastomosis) is created followed by a by a proximal right pulmonary artery to right atrium anastomosis, thus bypassing the defective ventricle.[8] Overtime this procedure has evolved and the second stage is now performed with an extracardiac conduit-total cavopulmonary connection (EC TCPC), often created using a synthetic conduit that connects the inferior vena cava (IVC) to the right pulmonary artery.[8,9] Use of an EC TCPC avoids atrial manipulation, which has been shown to reduce the incidence of

intractable arrhythmias compared to the classic Fontan operation.[10] Use of the Fontan procedure has significantly improved outcomes for patients with single ventricle cardiac anomalies resulting in a 73% survival rate at 15 years. In contrast, these defects are associated with a 70% mortality rate within the first year of life if left untreated.[11,12] Despite improvement, there remains significant long term morbidity associated with synthetic conduits. [13] The lack of growth potential in synthetic grafts results in delayed treatment and graft oversizing, both of which increase complications and impair growth and development of the patient.[14-17]

Similarly, MOS is a rare condition within the pediatric population that is characterized by severe narrowing of the abdominal aorta with or without involvement of the renal and mesenteric vessels. It is associated with severe hypertension; without intervention it is generally fatal between 30 and 40 years of age.[3,4] Although MOS may be associated with multiple etiologies, treatment universally necessitates restoration of distal blood flow to the kidneys and lower extremities.[18] Past treatments have included angioplasty, bypass grafting, and patch aortoplasty.[19] As with the modified Fontan procedure, these treatments have been limited by the use of synthetic materials, which due to a lack of growth potential require initial oversizing or multiple procedures throughout the development of the patient. Ideally, autologous tissue that could grow with the child to adulthood would be used to replace the coarcted portion of aorta. Recently, a tissue expander has been used to generate a lengthy segment of aortic tissue for this purpose; however, this procedure requires a 9-month period of tissue expansion.[20] As with

single ventricle physiology CHD, delayed treatment is associated with poorer outcomes and increased morbidity.

A potential solution- Tissue Engineered Vascular Grafts:

To address the limitations and complications of current technologies, tissue engineered vascular grafts (TEVGs) have emerged as an alternative source of vascular conduits. In its most simplified form vascular tissue engineering is the implantation of a biodegradable scaffold—seeded with cells or unseeded—within a living host. The biodegradable scaffold initially serves as a site of cell attachment and neotissue formation while acting as a passive conduit for blood flow. Over time, the biodegradable scaffold loses mechanical strength while the neotissue begins to develop mechanical strength. The culmination is a neovascular conduit composed entirely of autologous tissue with an intima, media, and adventitia in the absence of any scaffold material.[21]

Recently, TEVGs composed of a (poly)glycolic acid scaffold coated with a 50:50 copolymer of ε-caprolactone and L-lactide (P[PC/LA]) and seeded with bone marrow derived mononuclear cells have been developed for the venous circulation. These grafts were evaluated in the second stage of the Fontan procedure as EC TCPC in a pilot clinical trial in Japan by Dr. Toshiharu Shinoka and colleagues with excellent results.[22-25] All implanted grafts remained patent without aneurysmal dilatation, graft infection, graft rupture, or ectopic calcification; however, the primary complication encountered was stenosis in 6 out of 25 patients. Three of these patients required balloon angioplasty and one required balloon angioplasty

with stent placement. All patients were successfully treated and there was no graft related mortality.[26] In order to better understand the molecular mechanisms and mechanics behind TEVG development, a murine model was developed for both venous and arterial grafts.[27] This murine model has been extensively validated in the venous circulation where seeded grafts faithful recapitulate the results seen in the aforementioned pilot clinical trial.[28-32]

Development of a TEVG for the arterial circulation has been more difficult due to the relatively demanding high-pressure pulsatile arterial flow. When scaffolds similar to those used in the pilot clinical study are implanted within the arterial circulation rather than the venous circulation they typically rupture within ten days, presumably due to inadequate neotissue development in the context of rapid scaffold degradation and high arterial pressures. Instead, TEVGs composed of (poly)lactic acid (PLA) scaffolds are used due to their relatively slower degradation rate. While these grafts develop mild dilation, they remain patent without rupture through one year of implantation. In addition the neovessel developed endothelial cell layers and concentric smooth muscle layers.[27,33]

Growth and Remodeling- Exploring vascular biomechanics:

Arteries respond to changes in mechanical loading through a process of growth (changes in mass) and remodeling (changes in structure) that tends to maintain nearly constant the preferred levels of stress. Termed "mechanical homeostasis," these mechanobiologic responses occur at multiple levels, from whole tissue down to cellular and subcellular structures.[34] For example, large arteries

regulate their lumen via endothelial cell – smooth muscle cell responses that maintain a wall shear stress of approximately 1.5Pa.[35] Similarly, fibroblasts cultured in 3D collagen matrices generate an endogenous tensile stress and subsequently relax or contract to maintain this stress secondary to exogenous mechanical loading or unloading of the matrices.[36] Indeed, even pathologic situations such as aneurysms, which alter the hemodynamic loading, result in significant remodeling of extracellular matrix, via increased matrix metalloproteinase (MMP) activity and synthesis of collagens type I and III, which again appears to seek to return wall stresses toward normal levels.[37-39]

Nevertheless, the mechanobiology of neotissue formation has not been well explored in the field of vascular tissue engineering, wherein the focus is generally on gross mechanical metrics (e.g., burst pressure) or molecular biology (e.g., cytokine activity) independent of mechanical stimuli. Because a degradable polymeric scaffold, such as a TEVG, can exhibit changing mechanical properties that result in changes in the hemodynamics and the axial loads exerted on the host vessel, there is a pressing need to correlate the evolving cell and matrix biology with the evolving mechanics. Indeed, the radical change in mechanical environment that an interpositional TEVG introduces necessitates evaluation of the adaptive response of the adjacent artery.

Questions remaining to be answered:

An understating of the mechanobiology of native arteries has led to the development of computational models that predict arterial growth and remodeling (G&R) in response to changes in blood pressure, flow, and axial loading.[40-42] Evaluation of TEVGs implanted in the venous circulation has demonstrated evolving mechanical properties of TEVGs that approach that of native tissue by 24 weeks.[43] An associated modeling study by Miller and colleagues captures salient aspects of the biomechanics of the aforementioned venous remodeling.[44] Likewise, a G&R framework has been introduced to simulate TEVGs grown in bioreactors.[45] As of yet, there is insufficient experimental data with which to evaluate the mechanical development of arterial TEVGs or with which to generate computational models. Were such computational models to be developed, they could be a powerful tool, allowing for refinement and optimization of TEVGs *in silico* prior to more time intensive *in vivo* studies.

Statement of Purpose:

This project was designed to elucidate the mechanics by which arterial TEVGs develop and remodel. Specific emphasis was placed on comparing the mechanical development of the TEVGs with corresponding histologic and immunohistochemical development.

Hypothesis:

Bone marrow-derived mononuclear cell seeded TEVGs develop mechanical properties mimicking those of native arteries as their initial scaffold material is replaced by the cellular and extracellular components of the arterial wall.

Specific Aims:

1) Track biomechanical changes that occur as the TEVGs develop in the arterial circulation.

2) Track the histologic changes that occur as TEVGs develop in the arterial circulation.

METHODS:

This study was in accordance with the institutional guidelines for the care and use of laboratory animals, and the institutional committee approved the experimental procedures described below.

Graft Fabrication and Implantation:

TEVG scaffolds were constructed from sheets of nonwoven (poly)lactic acid (PLA; Concordia Fibers, Coventry, RI) that were rolled into a tube and sealed with a 50:50 copolymer of ε-(poly)caprolactone and L-(poly)lactide (P[PC/LA]; Absorbable Polymers International, Birmingham, AL) using a dual cylinder chamber molding system.[27] Briefly, a 5.0mm x 6.0mm PLA felt section was introduced through the inlet of the dual chamber system, while a 23-gauge stainless steel needle was then introduced into the opposing end to maintain the inner lumen. Afterward the 50:50 P[PC/LA] dissolved in glacial acetic acid was introduced followed by snap-freezing at -20°C for 30 minutes. The scaffold within the dual chamber device was lyophilized for 24 hours to eliminate solvents. Scaffolds were removed from the dual chamber device and trimmed to ~3.5mm in length, with an inner diameter of ~700μm and wall thickness of ~290μm (Fig. 1).

Prior to implantation, bone marrow derived mononuclear cells (BM-MNCs) were harvested from the tibia, femur, and humerus of 8-10 week old male C57BL/6 mice and isolated via density-gradient centrifugation using histopque-1077 (Sigma). The isolated cells were used to statically seed the scaffolds (~$1x10^6$ cells/scaffold)

by pipetting concentrated cells in media (RPMI-1640; Gibco, Inc.) into the inner lumen and outer surface of the scaffold.[28] Cells were incubated in RPMI-1640 for 12 hours at 37°C prior to implantation. Ethan Dean and Kevin Rocco aided the author in the bone marrow harvest and isolation of BM-MNCs.

The cell-seeded TEVGs were implanted as interpositional grafts in the infrarenal abdominal aorta (IAA) in 50 female CB57BL/6 mice between 8 and 10 weeks of age. Implantation was accomplished using a sterile microsurgical technique. Mice anesthetized with a peritoneal injection of ketamine and xylazine were placed in the supine position and opened with an abdominal midline incision. The IAA was exposed under magnification, cross-clamped, and excised. Scaffolds were inserted as interposition grafts using a running 10-0 nylon suture for the end-to-end proximal and distal anastomoses. All animal surgeries were performed by Dr. Tai Yi. The animals were recovered from surgery and maintained without the use of any anti-coagulation or anti-platelet therapy. [27]

Scanning Electron Microscopy:

Representative scaffolds were cut into 0.5mm thick cross-sections and imaged on a FEI XL-30 scanning electron microscope (SEM) [Hillsboro, OR]. Lumen diameters and wall thickness were measured from high magnification SEM images. Preparation of scaffolds for SEM and imaging was performed by Kevin Rocco.

Figure 1:

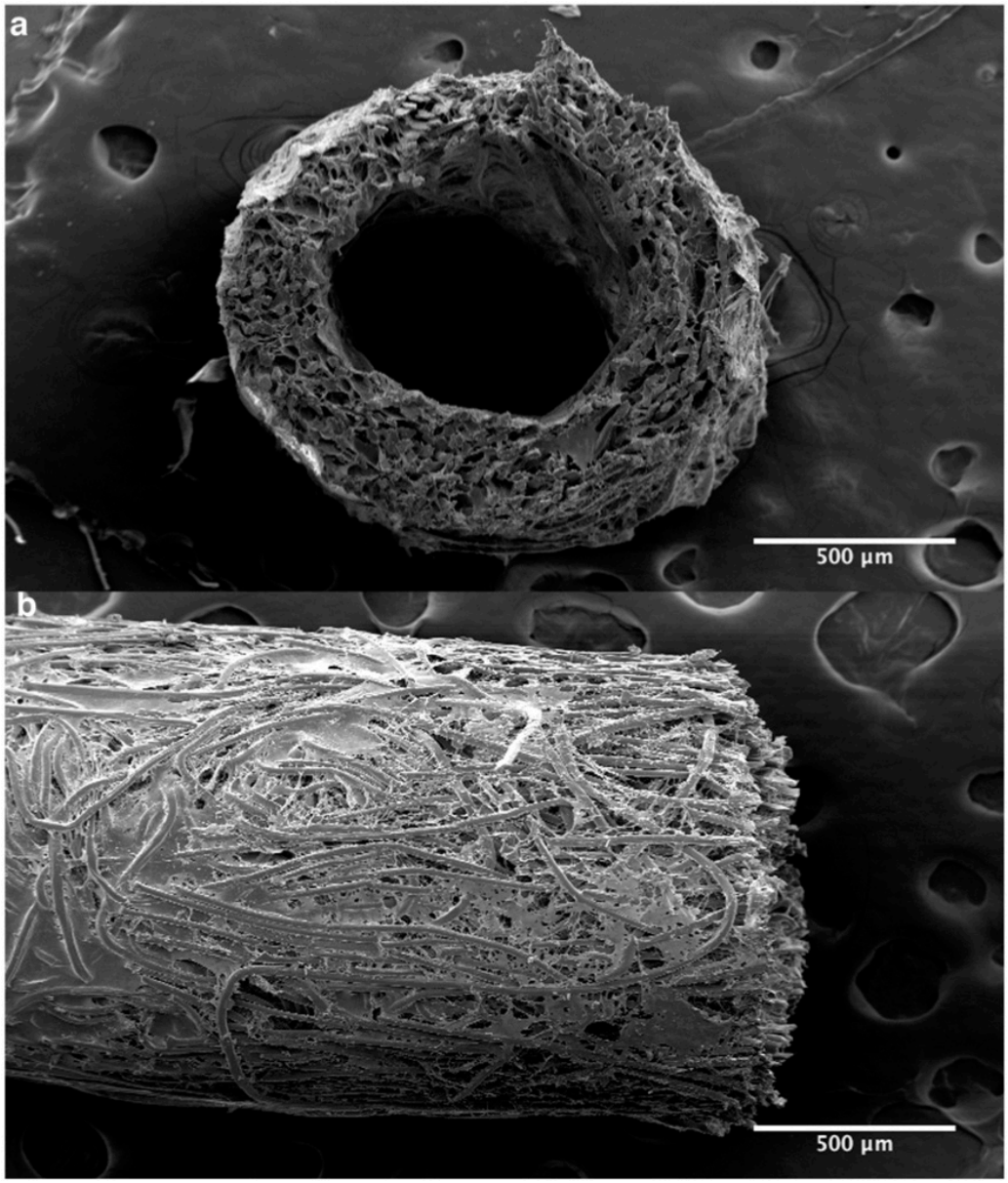

Figure 1: Scanning electron microscopic image of a representative pre-implant TEVG showing both a cross-sectional (*a*) and a longitudinal (*b*) section.

***In vivo* Ultrasound:**

TEVG patency, wall thickness, and luminal diameter were assessed *in vivo* while mice were sedated with isoflurane using high frequency ultrasound system (Vevo 770, Visualsonics, Toronto, Canada) with an RMV-704 transducer.

Biaxial Mechanical Testing:

At 3 and 7 months, TEVGs were harvested for biaxial mechanical testing. Following anesthesia using a peritoneal injection of ketamine and xylazine, a continuous vascular segment was harvested containing the TEVG as well as native IAA both proximally and distally. The author along with Ramak Khosravi preformed all explanations. Prior to explant, India ink was use to mark the proximal IAA, proximal TEVG, distal TEVG, and distal IAA. In order to ensure adequate pressurization and to prevent leakage during *in vitro* testing, branching vessels were identified and ligated. Photographs were taken to record the positions of the ink marks before explant and 10 minutes thereafter. Distances between marks were calculated with ImageJ software and used to determine the ratio between loaded and unloaded length, also known as *in vivo* axial stretch. After explant, the composite vessel was cannulated and secured to custom drawn micropipettes with 6-0 suture. The cannulated vessels were placed within a custom computer-controlled biaxial testing device described by Gleason et al. [46] The testing chamber was filled with Hank's balanced salt solution, including calcium chloride and magnesium chloride (Gibco, Inc.) (Fig. 2).

Figure 2:

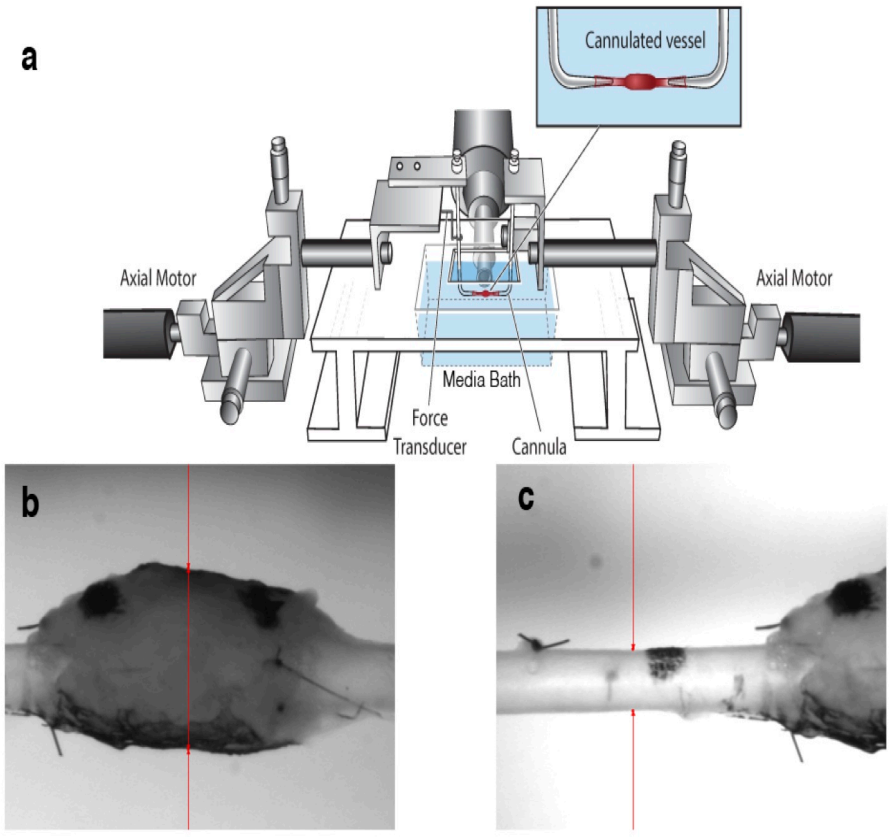

Figure 2: Schematic drawing of the biaxial mechanical testing device. (*a*) The composite vessel, consisting of the proximal IAA-TEVG-distal IAA, was cannulated using custom micropipettes. Luminal flow and pressure were controlled through the micropipettes and axial stretch was controlled via paired stepper motors; pressure and force were monitored with standard transducers. (*b*) Representative image of a TEVG mounted within the device with the video camera used for measuring diameter focused on the TEVG. (*c*) Representative image of a TEVG within the device with the camera focused on the proximal IAA. Outer diameter is indicated by the red arrows.

The composite vessels (proximal IAA—TEVG—distal IAA) were placed within the device at their unloaded state and initial unloaded dimensions were recorded. Prior to testing, vessels were allowed to equilibrate at 80 mmHg for 15 minutes at their measured *in vivo* axial stretch. The vessels were then preconditioned at this axial stretch by 4 cycles of pressurization from 10 to 100 mmHg at a rate of ~2 mmHg/second. Following preconditioning, unloaded dimensions were measured again; increases in dimensions relative to those taken prior to preconditioning and equilibration were minimal. The *in vivo* axial stretch of the composite vessel was also estimated *in vitro* by identifying the axial stretch at which axial force remained nearly constant in response to changes in luminal pressure.[47] This estimation was accomplished by measuring axial force at pressures of 50 mmHg, 60 mmHg, 80 mmHg, and 100 mmHg at axial stretches slightly above and below the value of axial stretch measured from the India ink dots. With the camera focused on the central region of the TEVG, pressure-diameter testing consisted of cyclic pressurization from 10 to 100 mmHg at the experimentally determined *in vivo* axial stretch and at ±5% this value. Pressure-diameter testing was repeated with the camera focused on the proximal IAA. Luminal pressure, axial force, outer diameter, and overall axial length were measured continually throughout testing using a custom LabView program.

Histology and Immunohistochemistry:

Samples explanted at 3 and 7 months were fixed in 10% neutral buffered formalin for 24 hours and embedded in paraffin.[28] Samples were stained with

hematoxylin and eosin (H&E), Masson's Trichrome (TRI), picrosirius red (PSR), Movat's Pentachrome (MOV), and Verhoeff-Van Gieson (VVG). VVG and TRI stained samples were analyzed with a custom Matlab code that quantifies pixels associated with elastin and collagen, respectively. The Matlab code was developed by Matthew Bersi. A similar program was used to calculate the relative distribution of large and small collagen fibers on PSR-stained sections. Unstained samples used for immunohistochemistry (IHC) were rehydrated and blocked for endogenous peroxidase activity; antibodies included those for CD31 (endothelial cell marker; Abcam), α-smooth muscle actin (Dako), calponin (Abcam), F4/80 (marker for mouse macrophages; AbD Serotec), MMP-2 (Abcam), MMP-9 (Abcam), collagen type I (Abcam), and collagen type III (Abcam). Antibody binding was detected using biotinylated secondary antibodies, followed by binding of streptavidin horseradish peroxidase[31] by the author with assistance from Ethan Dean. For immunofluorescence detection, tropoelastin (elastin marker; Abcam) was used with subsequent 4′,6-diamidino-2-phenylindole nuclear counterstaining[28] and performed by the author with assistance from Angela Huang.

Partial Collagenase Treatment:

Similar to Collins et al.[48], the lumen of the unloaded composite vessels, containing proximal IAA, TEVG, and distal IAA, was perfused with collagenase (1035 U/ml; Worthington Biochemical Corporation). This collagenase, which was tinted brown, remained intraluminal until collagen degradation allowed slow leaking from the IAA into the testing bath. At this point the mechanical integrity of the native IAA

was compromised, but the TEVG could still be pressurized. The TEVG was thus isolated immediately from the IAA, cannulated, washed with phosphate buffered saline (PBS), and subjected again to cyclic pressure-diameter testing at its cannulated stretch though a pressure range of 10 to 100 mmHg.

Elastase Treatment:

Similar to Ferruzzi et al. [49] and Collins et al. [48], the lumen of the composite vessels was perfused with 3 ml of elastase (7.5 U/ml; Worthington Biochemical Corporation) while maintained at its experimentally determined *in vivo* axial stretch. The elastase perfusion was maintained at 80 mmHg for 30 minutes, after which the dilatation of the proximal and distal IAA remained unchanged and any remaining elastase was washed out with media. Pressure-diameter testing was performed again on the composite vessel (i.e., TEVG and proximal IAA) at the original *in vivo* axial stretch and ±5% this value.

Statistical Analysis:

Pressure-diameter curves were normalized by dividing all outer diameter measurements by the minimum diameter at a given axial stretch and presented as mean ± standard error of the mean (SEM). All other data were represented as mean ± standard deviation (SD). Ultrasound data collected at multiple time points were analyzed by using two-way analysis of variance (ANOVA) with repeated measures, followed by Sidak's multiple comparisons test. All other data between groups were

analyzed using either a Student's t-test or one-way ANOVA, followed by Tukey's multiple comparisons test. P-values < 0.05 were considered statistically significant

Results:

In vivo Monitoring:

Fourteen of the fifty mice implanted (28%) were euthanized or died prematurely due to graft related complications (Fig. 3 *a* and *b*). Three distinct periods of failure were observed: (Early) within hours post-implant due to complications of micro-surgery (2%); (Intermediate) between 5 and 14 days due to failure of the P[PC/LA] sealant with resulting rupture along the seam on the scaffold (18%); (Late) between 14 days and 42 days due to rupture of the wall of the TEVG (8%). No graft related mortality occurred after 42 days and overall survival was 72%. On Doppler ultrasound, surviving mice had an increased luminal diameter within the TEVG when compared to native aorta, which was consistent with slight over-sizing of TEVG lumen at implantation. Wall thickness of TEVGs was also significantly greater than native aorta. Over the experimental time course, the TEVGs demonstrated stability in both luminal diameter and wall thickness without any statistically significant changes between 2 and 24-weeks (Fig. 3).

Biaxial Mechanical Testing:

A statistically significant difference was observed between axial stretch of the TEVG and IAA at both 3 and 7 months; however, no difference was observed

between time points (Fig. 4 *a* and *b*). Pressure-diameter curves of mounted composite vessels demonstrated a lack of compliance in TEVG compared to proximal IAA over a pressure range of 10 to 100 mmHg at both times (Fig. 5). Note, too, that the composite vessel maintained nearly constant axial force during pressure-diameter testing at the experimentally determined *in vivo* axial stretch (Fig. 4*c*).

Figure 3:

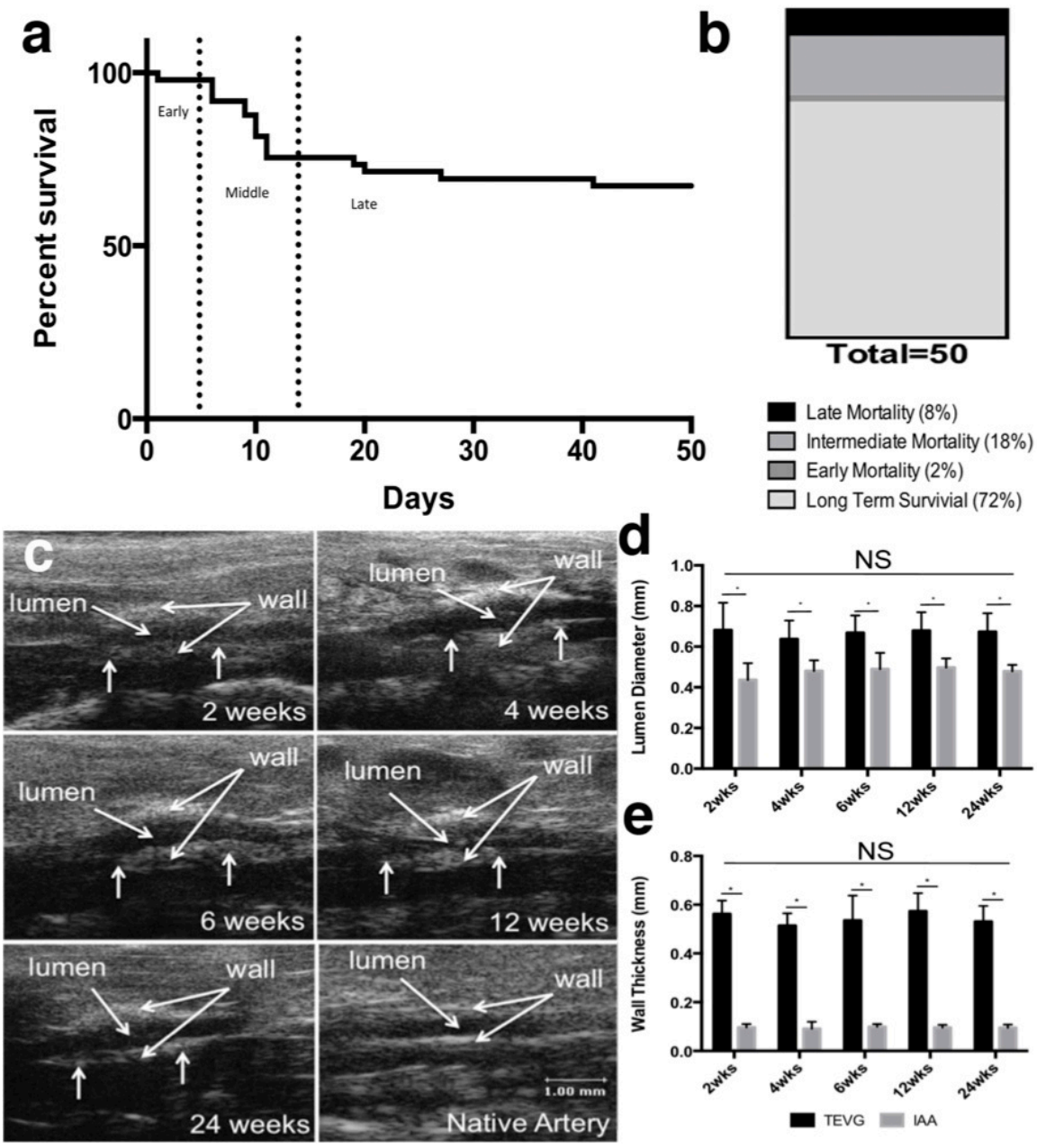

Figure 3: Survival and *in vivo* evaluation of TEVGs. (*a*) Survival curve demonstrating three distinct periods of mortality: early, intermediate, and late. (*b*) Percentage of long-term survival and mortality. (*c*) Representative Doppler ultrasound images of TEVGs at various times, which show consistent graft patency. (*d*) TEVG luminal diameter as measured by Doppler ultrasound (n=12). (*e*) TEVG wall thickness as measured by Doppler ultrasound (n =12). Data in graphs are expressed as mean ± SD. * $p < 0.05$; NS indicates statistically non-significant difference.

Figure 4:

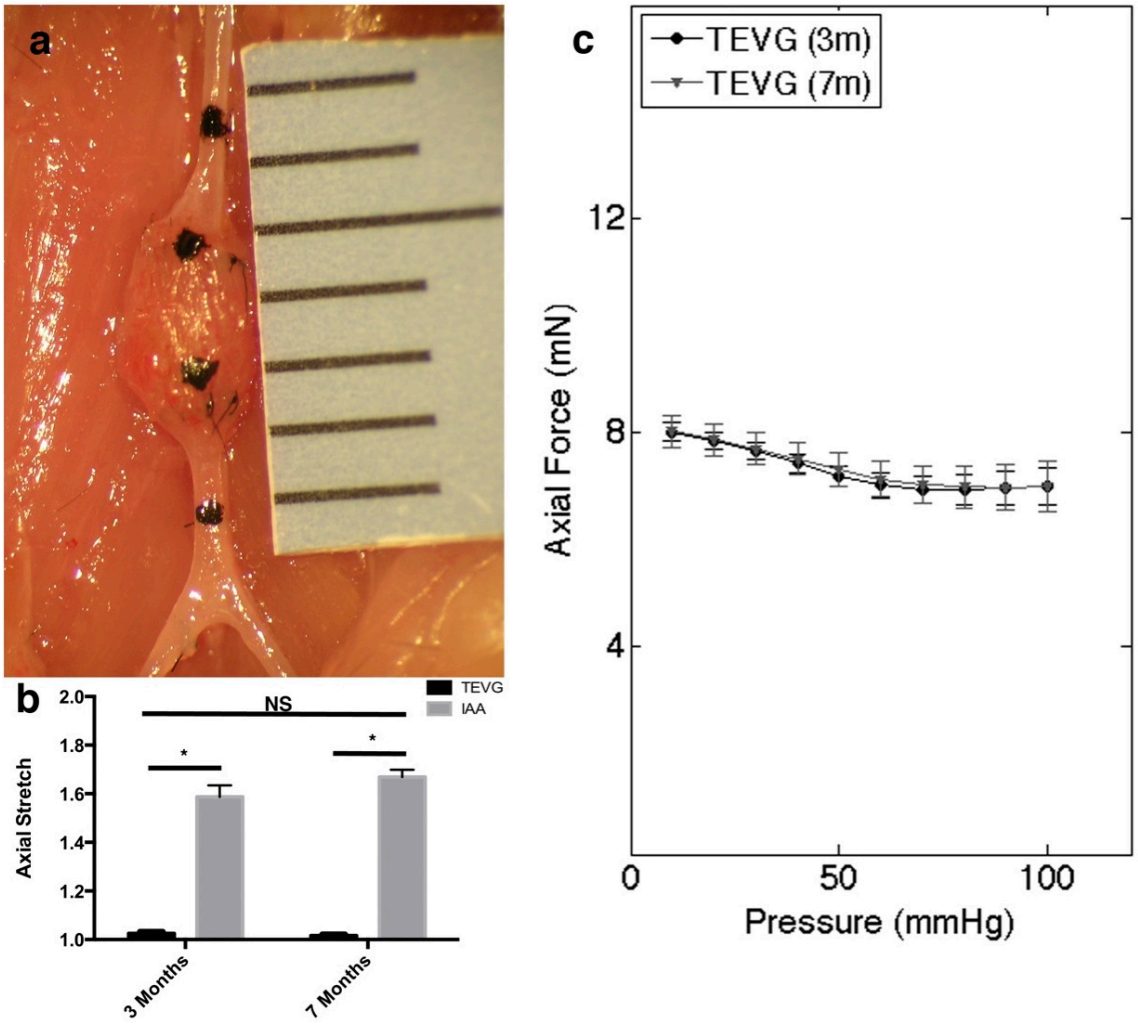

Figure 4: Evaluation of axial stretch and force. (*a*) Representative image of TEVG at explant. Note: India ink marked proximal IAA, proximal TEVG, distal TEVG, and distal IAA. (*b*) Axial stretch ratio of the loaded and unloaded state measured at 3 (n=9) and 7 (n=6) months expressed as mean ± SD. (*c*) Axial Force during pressure-diameter curves at 3 and 7 months at *in vivo* axial stretch expressed as mean ± SEM. * $p < 0.05$; NS indicates statistically non-significant difference.

Figure 5:

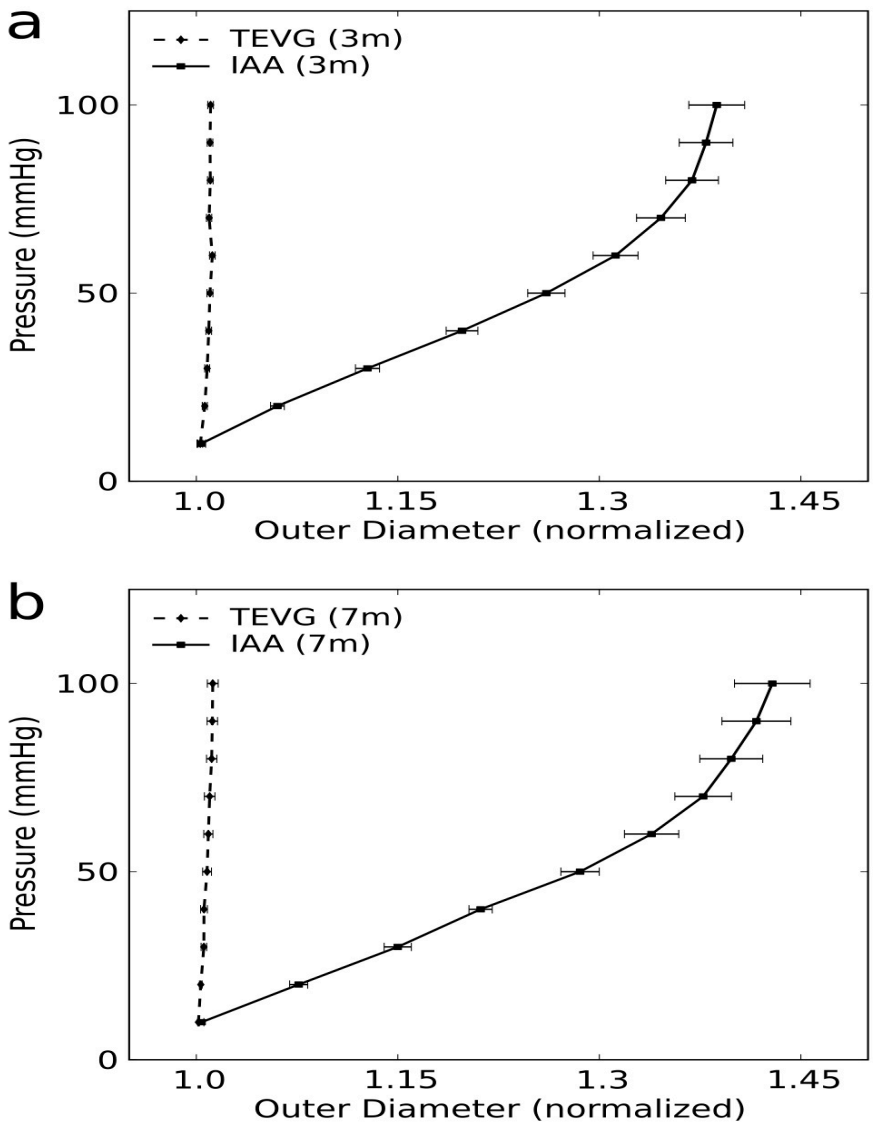

Figure 5: Pressure-diameter curves at (*a*) 3 months (*n*=9) and (*b*) 7 months (*n*=6) comparing proximal IAA and TEVG at *in vivo* axial stretches. Data in graphs are expressed as mean ± SEM.

TEVGs develop endothelial cell lining and smooth muscle layers:

Histologic analysis revealed extensive cellular infiltration within the TEVGs (Fig. 6). TEVGs had increased luminal diameter and wall thickness relative to native IAA harvested from aged-matched controls. The difference in luminal area appeared more pronounced on histologic staining than on ultrasound, likely due increased recoil and dehydration effects during fixation in the native tissue. H&E staining showed abundant residual polymer at both times, which could be isolated and quantified under polarized light due to innate birefringence (Fig. 8*r*). Immunohistochemical staining for CD31 indicated development of a luminal endothelial layer, while staining for calponin and α-smooth muscle actin indicated the presence of smooth muscle cells within the wall. Note that positive staining for calponin occurred predominantly in concentric neotissue layers between the polymer and endothelialized lumen. The presence of extensive macrophages on F4/80 staining suggested an inflammatory component to the remodeling process, which was further characterized by the positive staining of MMP-2 and MMP-9 at 3 months. MMP-2 staining persisted at 7 months, while MMP-9 was decreased (Fig. 7).

Figure 6:

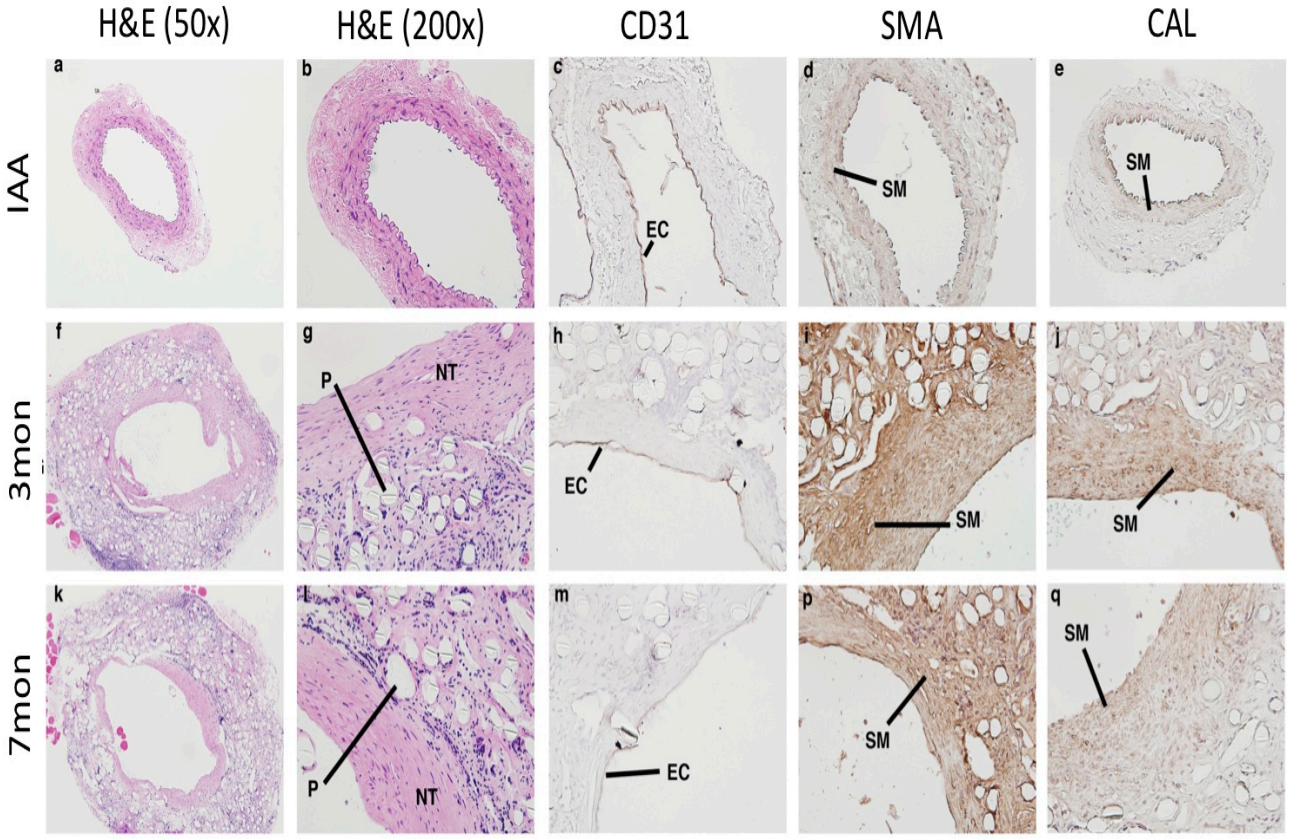

Figure 6: Morphologic evaluation of mouse IAA and TEVG at 3 and 7 months post-implantation. Native mouse IAA stained for (*a-e*): H&E (cell nuclei), CD31 (endothelial cells (EC)), and SMA and CAL (smooth muscle (SM)). Similarly, TEVG at 3 months (*f-j*) and 7 months (*k-q*) stained for: H&E, CD31, SMA, and CAL. Note the abundant residual polymer (P) in the TEVG, with the neotissue (NT) forming along the lumen. Low-magnification photomicrographs are at magnification of 50x. All other photomicrographs are at a magnification of 200x.

Figure 7:

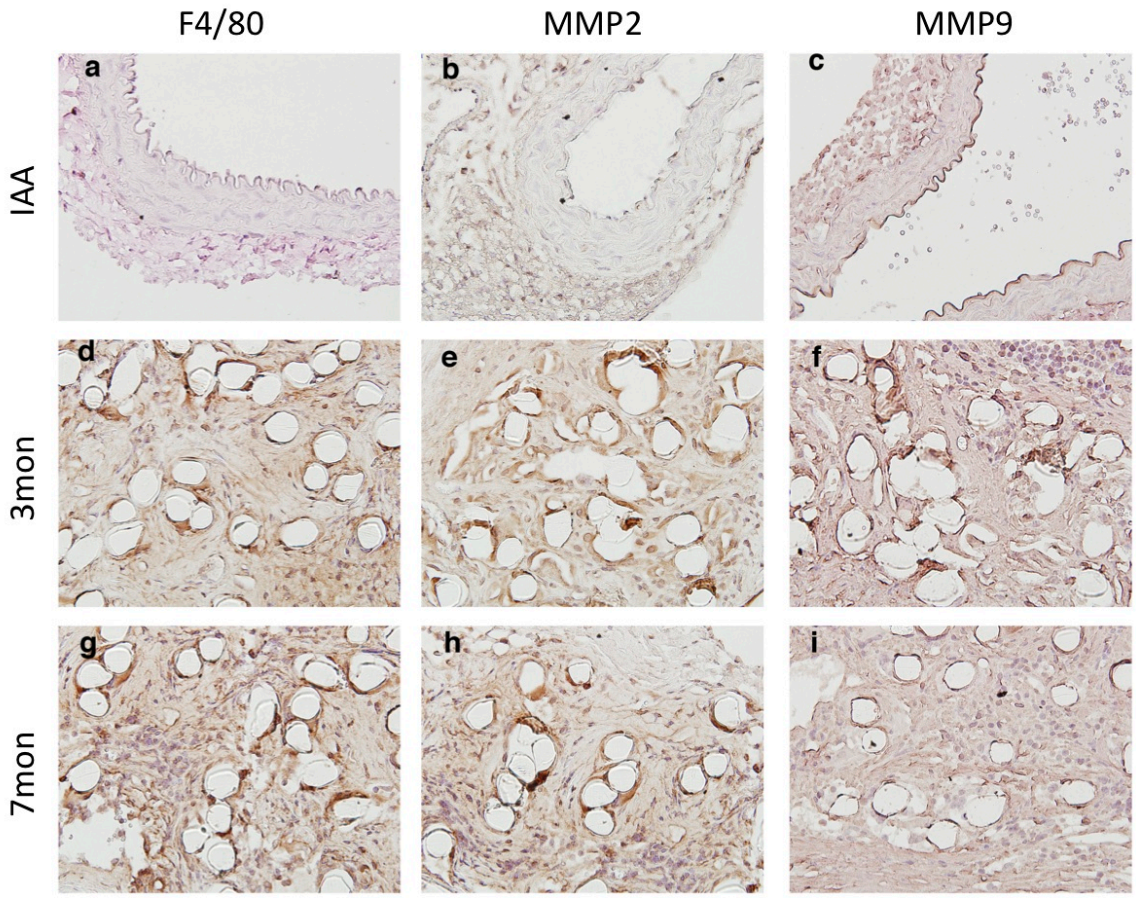

Figure 7: Evaluation of inflammatory response to TEVG. Native mouse IAA stained for (*a-c*): F4/80 (mouse macrophage marker), MMP-2, and MMP-9. Similarly, TEVG at 3 months (*d-f*) and 7 months (*g-i*) stained for F4/80, MMP-2, and MMP-9. All photomicrographs are at a magnification of 300x.

Collagen Contributes to TEVG Stiffness:

Extensive deposition of collagen was demonstrated by TRI staining (Fig 8). Quantification of pixels positive for collagen revealed similar area fractions for collagen between native IAA and TEVG at both 3 and 7 months. PSR, which provides information on the diameter of the collagen fibers, revealed a similar pattern of distribution of large (red/orange) and small (yellow/green) fibers between native IAA and TEVG at both low and high light exposure (Fig. 9). The low light exposure was used to focus on the adventitia while the high light exposure was used to focus on the media. Collagen content of TEVGs was further characterized by IHC, which revealed collagen type I (COL I) and collagen type III (COL III) throughout the TEVG wall, both closely associated with areas containing residual polymer.

Whereas complete enzymatic degradation of collagen caused the TEVG to leak, partial treatment with collagenase maintained structural integrity. Pressure-diameter testing at 3 and 7 months demonstrated a modest increase in TEVG compliance due to partial loss of collagen, hence implying some contribution of collagen to the circumferential stiffness that was dominated by polymer post-treatment (Fig. 10).

Figure 8:

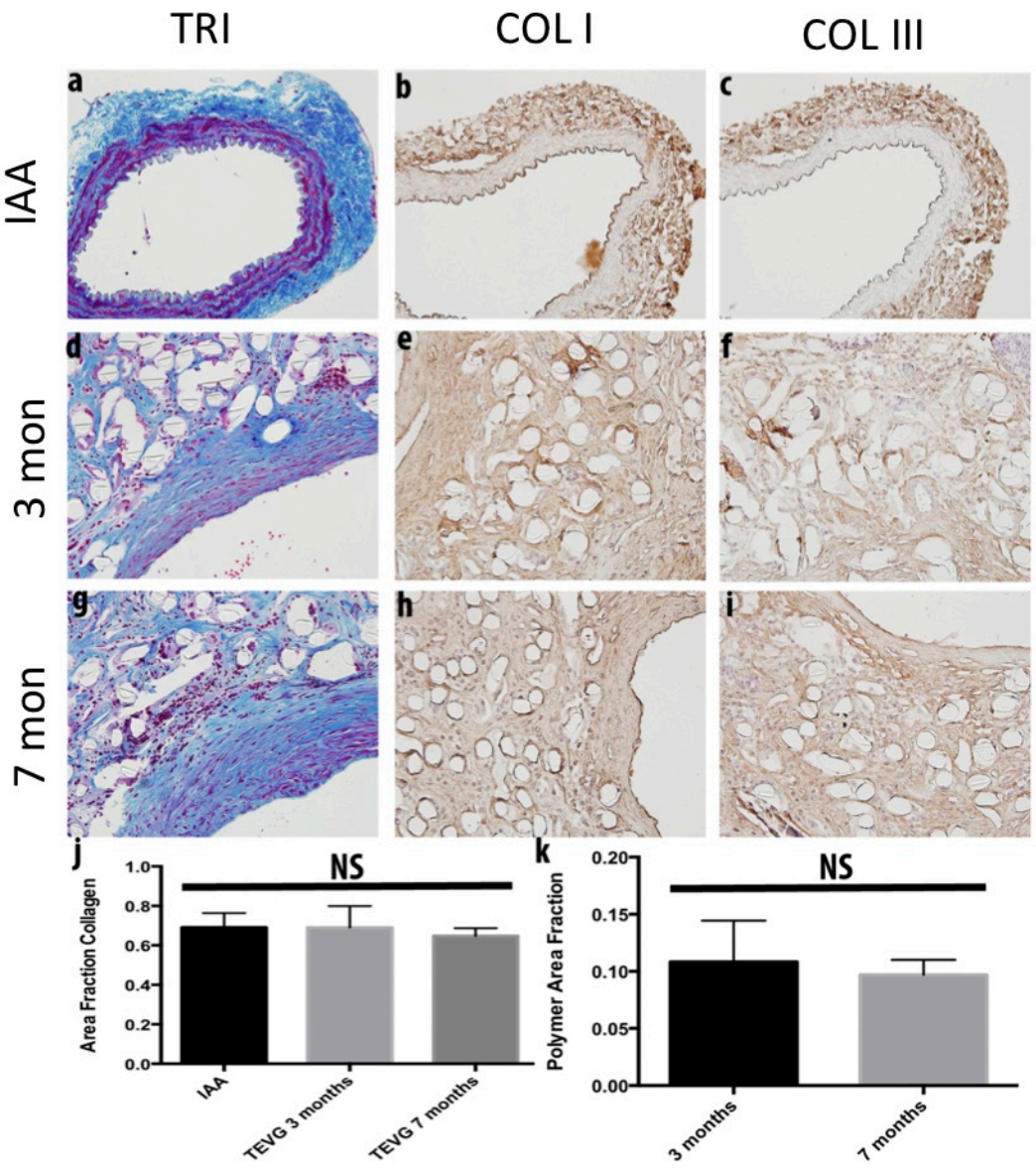

Figure 8: Quantification of collagen within TEVG. Native mouse IAA stained with (*a-c*): TRI, COL I, and COL III. Similarly, TEVG at 3 months (*d-f*) and 7 months (*g-i*) stained for TRI, COL I, and COL III. (*j*) Evaluation of area fraction of collagen within biologically active stained tissue for TRI stain. (*k*) Evaluation of residual polymer within TEVG at 3 and 7 months. All photomicrographs at magnification of 200x. Data in graphs are expressed as mean ± SD (n=4 for all groups; all differences between groups was statistically non-significant (NS)).

Figure 9:

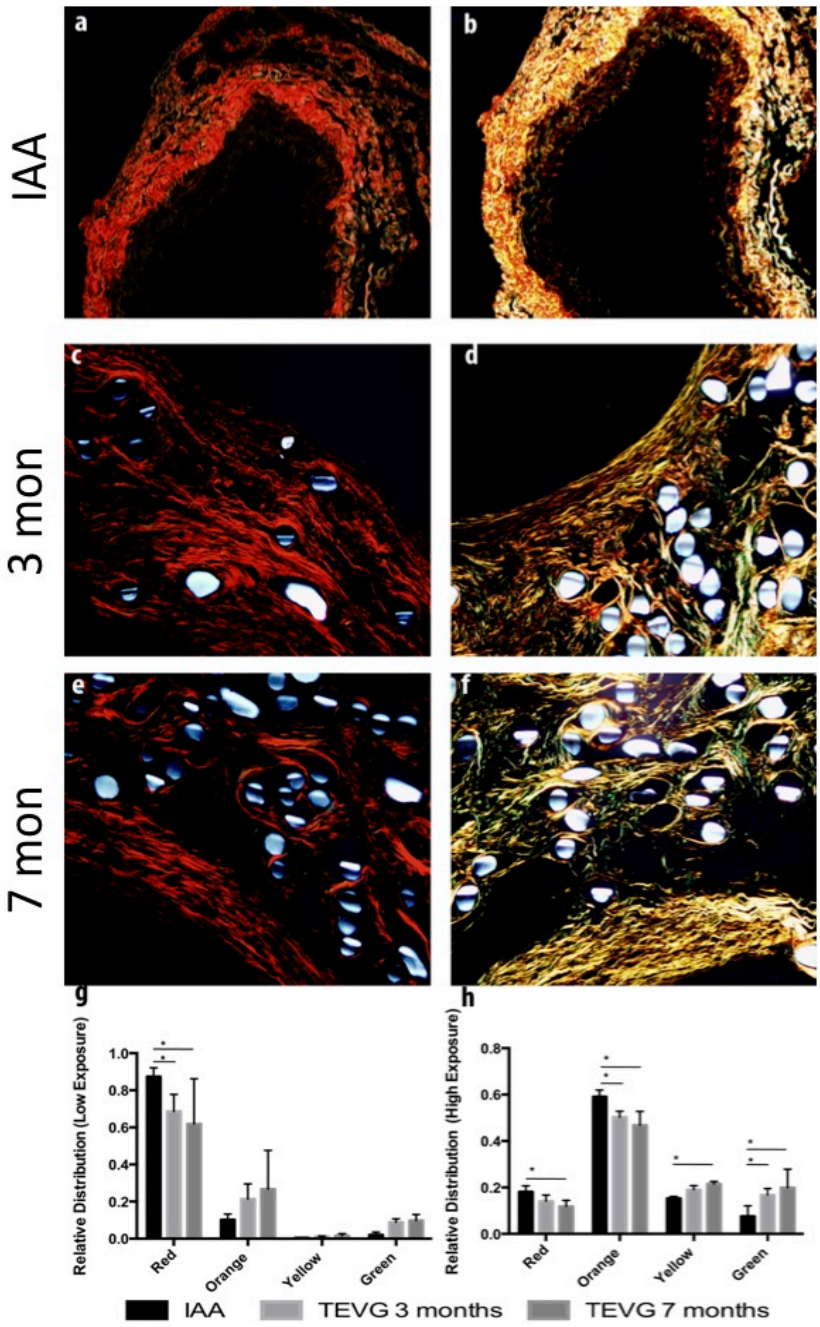

Figure 9: Evaluation of collagen fiber size within TEVG. Native mouse IAA stained with (*a-b*) PSR focused on adventitia (PSR ADV), PSR focused on media (PSR MED). Similarly, TEVG at 3 months (*c-d*) and 7 months (*e-f*) stained for PSR focused on adventitia and PSR focused on media. (g) Relative percentage of large diameter and small diameter fibers by PSR staining at low light exposure (adventitia). (*h*) Relative percentage of large diameter and small diameter fibers by PSR staining at high light exposure (media). *$p < 0.05$

Evaluation of Elastin:

By 3 months, elastin was evident along the inner circumferential layers of the TEVG (Fig. 10). Using a digital extraction method and VVG staining, we found a significant increase in the area fraction of elastin between 3 and 7 months. Nevertheless, the elastin fraction was significantly lower than native at both times. In addition, the elastic fibers in the TEVG appeared thinner and less organized than those in native tissue, most notably on immunohistochemical staining of tropoelastin (Fig. 11). At both 3 and 7 months, treatment with elastase did not significantly change TEVG compliance (Fig. 10). Conversely, the elastase did decrease the compliance of the proximal IAA, which then mimicked the appearance of the TEVG pressure-diameter curves.

Figure 10:

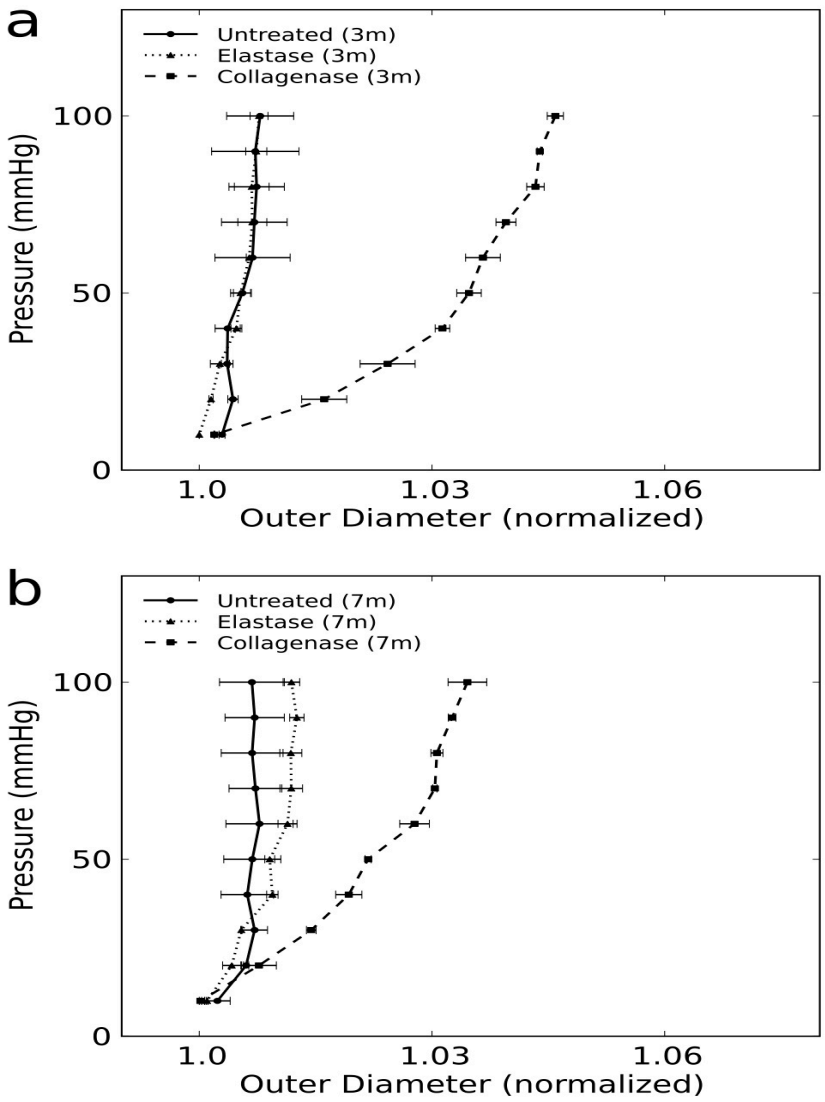

Figure 10: Pressure-diameter curves for untreated (n=4), elastase treated (n=2), and partial-collagenase (n=2) treated TEVGs at (a) 3 months and (b) 7 months. Data in graphs are expressed as mean ± SEM.

Figure 11:

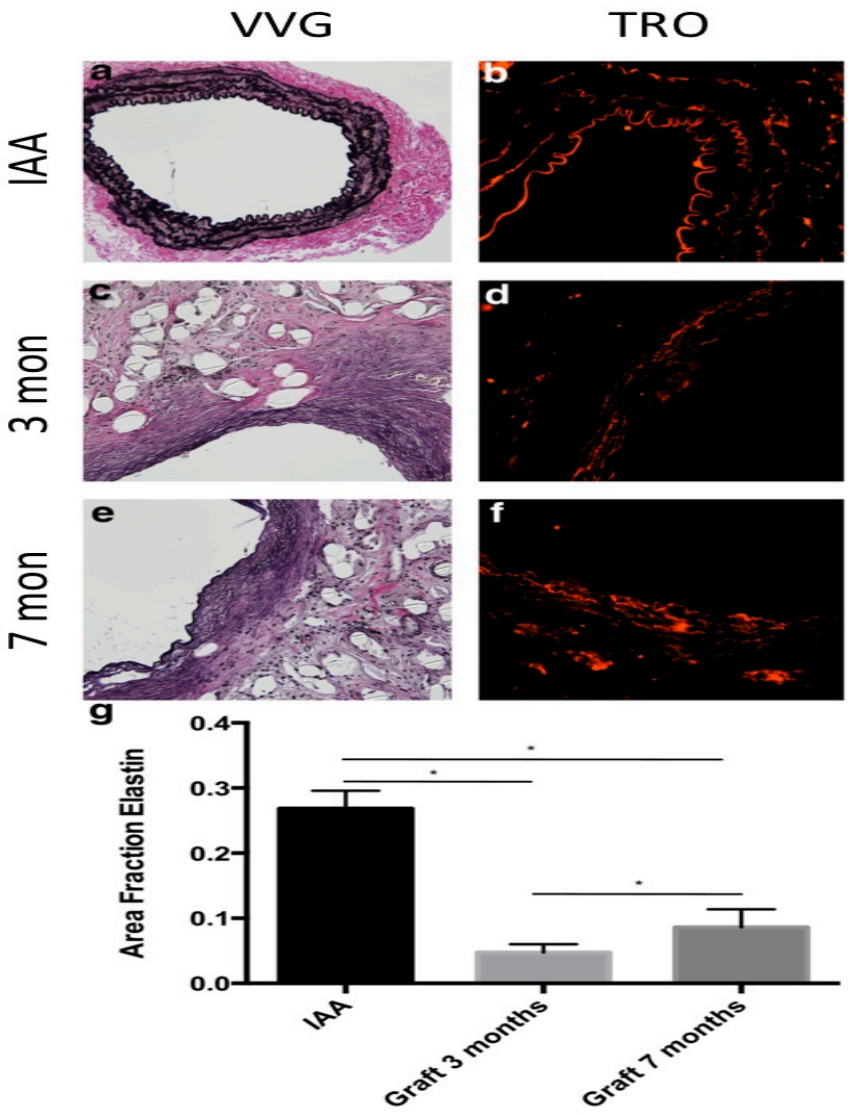

Figure 11: Evaluation of elastin fiber development within TEVGs. Native mouse IAA stained for (*a* and *b*): VVG (elastic fibers) and TRO. Similarly, TEVG at 3 months (*c* and *d*) and 7 months (*e* and *f*) stained for VVG and TRO. (*g*) Area fraction of elastin within biologically active stained tissue by VVG stain (n=4 for all groups). VVG and TRO photomicrographs are at a magnification of 200x and 300x respectively. Data in graphs are expressed as mean ± SD. *p <0.05

Discussion:

This study was designed to assess evolving biomechanical properties of TEVGs implanted in the arterial circulation and to begin to elucidate mechanobiological principles that affect vascular neotissue formation. Within the past five years, several arterial grafts have been evaluated in both mouse and rat models.[33,50-52] While the field has shown rapid advancement in the creation of autologous blood vessels with the potential to function as vascular grafts, little is known about the mechanical properties of these engineered constructs as they mature within their host recipients. It is hoped that an understanding of mechanobiologic principles can be exploited in the rational design of an improved TEVG, including via the use of associated computational models.

Although TEVGs designed for the venous circulation achieved success in a pilot clinical study, arterial TEVGs lag behind primarily due to the difficulties of creating a degradable scaffold that can withstand pulsatile high-pressure arterial blood flow. Clinical translation of arterial TEVGs has been achieved only by McAllister and colleagues with sheet based TEVGs used as arteriovenous shunts for hemodialysis in patients with end stage kidney disease.[53] While initially successful, complications were encountered in the 3 out of 10 patients who developed graft thrombosis, dilation, and aneurysm respectively.[54] Moreover, the cell sheet technique required several weeks to mature in culture prior to implantation.[55] Due to these limitations it remains unclear if a cell sheet based TEVG would be suitable in the pediatric population where delayed intervention can result in increased

morbidity. Recent work by the same group using allogeneic cells to grow a TEVG prior to implantation has shown promise. Through this method, TEVGs were created from allogeneic sheets of fibroblasts and then stored for several months prior to implant. In this way the pre-made TEVGs came closer to achieving an "off-the-shelf" potential. However, the clinical translation of this technique is in early stages and complications have arisen in 2 of the 3 patients receiving grafts.[56] In contrast, the work described herein utilizes a same day seeding and implantation method similar to that used in venous TEVGs that have proven efficacious in a pilot clinical study.[25,26]

Vascular neotissue formation describes the process by which a biodegradable scaffold transforms into a living vascular conduit, whether initially seeded with cells or not. As the scaffold degrades, neotissue forms and ultimately gives rise to a neovessel when the scaffolding is degraded completely. Despite significant advances in our understanding of mechanobiological factors affecting vascular biology in health and disease, there has been little research on these processes during neovessel formation. The biomechanical properties of the TEVG are initially determined exclusively by the properties of the tubular scaffold, but over time the cells begin to produce an extracellular matrix that increasingly contributes to the properties of the graft. As in native blood vessels, this extracellular matrix is composed primarily of collagen, elastin, and glycosaminoglycans. As the scaffold degrades, it is thought that the cells can sense the increased load borne by the deposited extracellular matrix, which it presumably remodels or refashions in an attempt to establish the aforementioned mechanical

homeostasis. At the point when the scaffold degrades completely, the extracellular matrix is necessarily the primary determinant of the biomechanical properties of the graft and hence both the overall structural integrity and its adaptive potential. Recent work by Naito, Lee, and colleagues demonstrated that developing venous TEVGs composed of an initially stiff (poly)glycolic acid scaffold develop increased compliance that approaches native IVC by 24 weeks after implantation.[43] This work has indicated a complex, time-dependent process in which collagen deposited during the first 12 weeks is replaced or remodeled into more compliant forms in the context of a fully degraded PGA scaffold. See, too, the associated modeling study by Miller and colleagues that captures salient aspects of the associated biomechanics.[44]

The present study was designed to determine if similar mechanobiological processes occur in neovessel formation within the arterial system and to generate mechanical data to serve as a foundation for the extension of the prior computational modeling to the arterial system. We found that, despite initial mortality associated with seam line rupture, arterial TEVGs were stable after 6 weeks with no aneurysmal dilation or stenosis. Similar to the work of Mirensky et al.[33], TEVGs developed a luminal endothelial cell layer as well as a smooth muscle cell populated "medial" layer. Structurally, our results revealed many of components of a normal extracellular matrix, including elastin and collagen types I and III.[57] MMP-2 and MMP-9 activity, along with extensive infiltration by macrophages, suggested an ongoing inflammatory mediated process of remodeling. This chronic inflammation likely resulted from the persistence of the PLA, which further contributed to the continued low compliance in both the circumferential and

axial directions. That is, the elastin found histologically played no mechanical role in overall TEVG performance while the collagen contributed only moderately to the stiffness. Hence, although the graft satisfied minimal mechanical requirements, such as sufficient suture retention and burst pressure, and clinical requirements, such as lack of stenosis or aneurysmal expansion, it clearly had not approached native structure or function by 7 months.

Not only are the properties of the TEVG important for its integrity and adaptivity, they are also important determinants of mechanobiological adjustments by the adjacent host vessels. Toward this end, we observed a persistent compensation by the native IAA in response to the high stiffness of the TEVG. At the composite vessel's *in vivo* axial stretch, a near constant force could be achieved through a range of pressures, similar to that of native arteries in the preferred homeostatic state.[58] Yet, the axial force in the composite vessels was lower by ~4 mN compared with the axial force in non-implanted IAA in C57BL/129sv mice[47]; likewise, there was a decreased compliance in the proximal IAA relative to normal (Fig. 12). Although differences in mouse backgrounds (pure versus mixed C57BL/6) and testing procedures (e.g., pressurization up to 100 mmHg rather than 140 mmHg) may have contributed to the observed differences, both differences seen in Fig. 12 likely resulted from the adjacent host aorta adapting to the stiff interpositional TEVG. Optimal design of TEVGs should clearly seek to minimize adverse adaptations in the host vessels.

Figure 12:

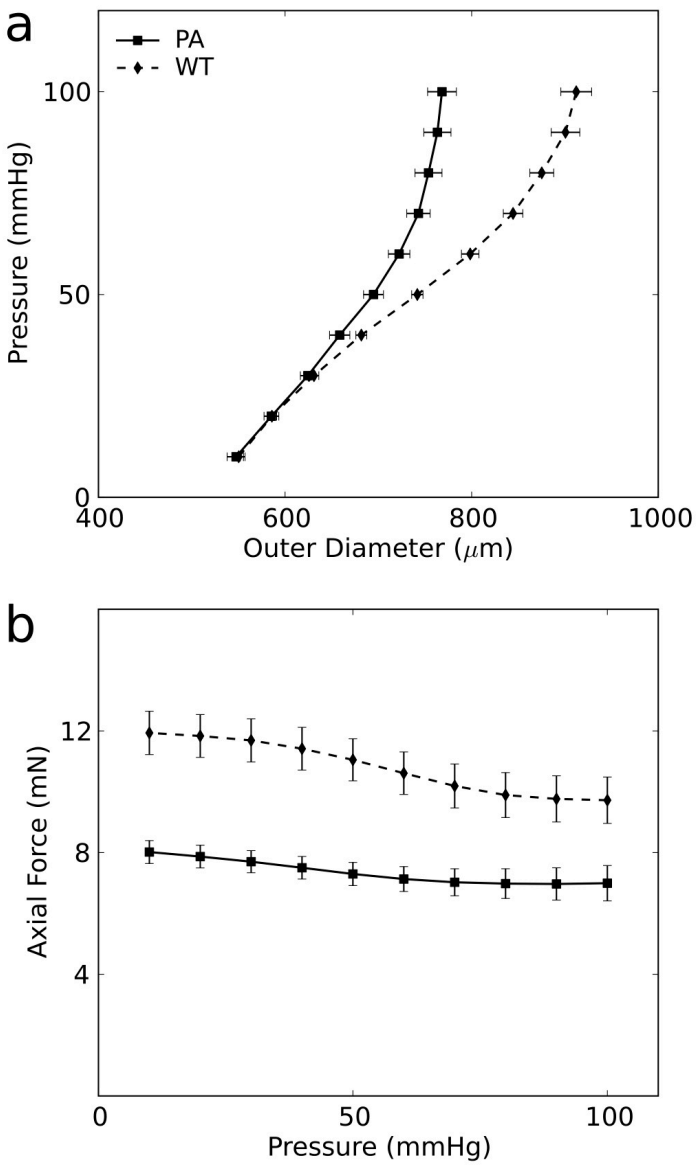

Figure 12: Comparison of IAA in mice with and without TEVG implant. Pressure diameter curve (*a*) and pressure-force curve (*b*) between non-implanted (WT) mice and proximal IAA (PA) in mice with TEVG implant at 7 months. Non-implanted data adapted with permission from Ferruzzi et al. Data in graphs are expressed as mean ± SEM.

This study is the first to examine the long-term structure and properties associated with neovessel formation in the arterial system. The data confirm the importance of overlapping inflammatory and mechanobiologically mediated matrix production seen before in venous TEVGs (cf. [44]). This work also highlights the importance of mechanical evaluations of evolving TEVGs that delineate effects of different matrix components as complements to traditional histological and biochemical analysis, for the mere presence of significant matrix need not imply significant load carrying capability. It is hoped that such data can inform computational models that can predict preferred time courses of polymer degradation and matrix incorporation within the evolving graft. Such models have the potential to decrease both the time and expense associated with purely trial and error experimental approaches to improving tissue engineered vessels and thereby to open the door for next generation rationally designed TEVGs.

While we did not see evolution of the mechanical properties of the PLA TEVGs examined in this study, all developed techniques can be readily applied to TEVGs composed of other scaffold biomaterials. The next steps in vascular tissue engineering for the arterial circulation will necessitate a reexamination of these biomaterials. A balance is needed between initial strength to prevent aneurysm and gradual degradation to encourage development of mechanically active extracellular matrix products. The results of this work show collagen production reaches a steady point by 3 months, thus suggesting that complete scaffold degradation by this time may be tolerated. New methods of scaffold production such as electrospinning offer one possibility. Electrospun scaffolds are generated using a

polymer solution that is ejected across a charged field that is grounded upon a spinning mandrel. In this way, a scaffold can be "spun" that contains no seam line and its initial properties such as fiber orientation and graft porosity can be manipulated by changing the rate of polymer ejection and scaffold rotation.[59] Recent *in vivo* results using this technique have been promising and have demonstrated biocompatibility of a number of polymer solutions.[60-65] Moreover, the lack of a seam line in electrospun scaffolds eliminates an inherent weakness in scaffolds composed of woven sheets that accounted for the vast majority of our mortality.

In summary, we report the first in depth examination of arterial TEVG mechanical properties and corresponding histologic properties at late term time points. These PLA-PCLA grafts performed well with the notable exception of seam line rupture in the early weeks after implantation. Although stable, these grafts did not demonstrate appreciable evolution of mechanical properties between 3 and 7 months. Using new techniques for evaluating individual contributions of collagen and elastin, with correlations with histologic and immunohistochemical results, we found that there was evidence of cellular and ECM development between these time points but no change in the ample residual PLA scaffolds. It is likely that this residual PLA played a key role in determining overall graft mechanics, and its long-term presence within the graft may impede graft development. Thus a reevaluation of initial scaffold material will be a crucial step in the development of arterial TEVGs. Fortunately with the advent of the described techniques that allow for computation of overall graft mechanics, it may be possible to evaluate these new materials *in*

silico, prior to *in vitro* and *in vivo* experimentation. Such computations could greatly accelerate next generation TEVG development and decrease the overall experimental cost.

References:

1. Go AS, Mozaffarian D, Roger VL, et al. Heart disease and stroke statistics--2013 update: a report from the American Heart Association. Circulation 2013;127:e6-e245.
2. Selvin E, Erlinger TP. Prevalence of and risk factors for peripheral arterial disease in the United States: results from the National Health and Nutrition Examination Survey, 1999-2000. Circulation 2004;110:738-43.
3. Lewis VD, 3rd, Meranze SG, McLean GK, O'Neill JA, Jr., Berkowitz HD, Burke DR. The midaortic syndrome: diagnosis and treatment. Radiology 1988;167:111-3.
4. Cohen JR, Birnbaum E. Coarctation of the abdominal aorta. J Vasc Surg 1988;8:160-4.
5. Goldman S, Zadina K, Moritz T, et al. Long-term patency of saphenous vein and left internal mammary artery grafts after coronary artery bypass surgery: results from a Department of Veterans Affairs Cooperative Study. Journal of the American College of Cardiology 2004;44:2149-56.
6. Conte MS. The ideal small arterial substitute: a search for the Holy Grail? FASEB journal : official publication of the Federation of American Societies for Experimental Biology 1998;12:43-5.
7. Udelsman BV, Maxfield MW, Breuer CK. Tissue engineering of blood vessels in cardiovascular disease: moving towards clinical translation. Heart 2013;99:454-60.
8. Fontan F, Baudet E. Surgical repair of tricuspid atresia. Thorax 1971;26:240-8.
9. Marcelletti C, Corno A, Giannico S, Marino B. Inferior vena cava-pulmonary artery extracardiac conduit. A new form of right heart bypass. The Journal of thoracic and cardiovascular surgery 1990;100:228-32.
10. Gewillig M, Wyse RK, de Leval MR, Deanfield JE. Early and late arrhythmias after the Fontan operation: predisposing factors and clinical consequences. British heart journal 1992;67:72-9.
11. Samanek M. Children with congenital heart disease: probability of natural survival. Pediatric cardiology 1992;13:152-8.
12. Hager A, Kaemmerer H, Eicken A, Fratz S, Hess J. Long-term survival of patients with univentricular heart not treated surgically. The Journal of thoracic and cardiovascular surgery 2002;123:1214-7.

13. Fontan F, Kirklin JW, Fernandez G, et al. Outcome after a "perfect" Fontan operation. Circulation 1990;81:1520-36.
14. Alexi-Meskishvili V, Ovroutski S, Ewert P, et al. Optimal conduit size for extracardiac Fontan operation. Eur J Cardiothorac Surg 2000;18:690-5.
15. Pearl JM, Laks H, Drinkwater DC, Capouya ER, George BL, Williams RG. Modified Fontan procedure in patients less than 4 years of age. Circulation 1992;86:II100-5.
16. Petrossian E, Reddy VM, McElhinney DB, et al. Early results of the extracardiac conduit Fontan operation. The Journal of thoracic and cardiovascular surgery 1999;117:688-96.
17. Ovroutski S, Ewert P, Alexi-Meskishvili V, et al. Comparison of somatic development and status of conduit after extracardiac Fontan operation in young and older children. Eur J Cardiothorac Surg 2004;26:1073-9.
18. Panayiotopoulos YP, Tyrrell MR, Koffman G, Reidy JF, Haycock GB, Taylor PR. Mid-aortic syndrome presenting in childhood. Br J Surg 1996;83:235-40.
19. Stanley JC, Criado E, Eliason JL, Upchurch GR, Jr., Berguer R, Rectenwald JE. Abdominal aortic coarctation: surgical treatment of 53 patients with a thoracoabdominal bypass, patch aortoplasty, or interposition aortoaortic graft. J Vasc Surg 2008;48:1073-82.
20. Kim HB, Vakili K, Modi BP, et al. A novel treatment for the midaortic syndrome. N Engl J Med 2012;367:2361-2.
21. Langer R, Vacanti JP. Tissue engineering. Science 1993;260:920-6.
22. Matsumura G, Miyagawa-Tomita S, Shin'oka T, Ikada Y, Kurosawa H. First evidence that bone marrow cells contribute to the construction of tissue-engineered vascular autografts in vivo. Circulation 2003;108:1729-34.
23. Naito Y, Imai Y, Shin'oka T, et al. Successful clinical application of tissue-engineered graft for extracardiac Fontan operation. The Journal of thoracic and cardiovascular surgery 2003;125:419-20.
24. Shin'oka T, Imai Y, Ikada Y. Transplantation of a tissue-engineered pulmonary artery. The New England journal of medicine 2001;344:532-3.
25. Shin'oka T, Matsumura G, Hibino N, et al. Midterm clinical result of tissue-engineered vascular autografts seeded with autologous bone marrow cells. The Journal of thoracic and cardiovascular surgery 2005;129:1330-8.
26. Hibino N, McGillicuddy E, Matsumura G, et al. Late-term results of tissue-engineered vascular grafts in humans. The Journal of thoracic and cardiovascular surgery 2010;139:431-6, 6 e1-2.
27. Roh JD, Nelson GN, Brennan MP, et al. Small-diameter biodegradable scaffolds for functional vascular tissue engineering in the mouse model. Biomaterials 2008;29:1454-63.
28. Roh JD, Sawh-Martinez R, Brennan MP, et al. Tissue-engineered vascular grafts transform into mature blood vessels via an inflammation-mediated process of vascular remodeling. Proc Natl Acad Sci U S A 2010;107:4669-74.
29. Hibino N, Villalona G, Pietris N, et al. Tissue-engineered vascular grafts form neovessels that arise from regeneration of the adjacent blood vessel. FASEB journal : official publication of the Federation of American Societies for Experimental Biology 2011;25:2731-9.

30. Hibino N, Yi T, Duncan DR, et al. A critical role for macrophages in neovessel formation and the development of stenosis in tissue-engineered vascular grafts. FASEB journal : official publication of the Federation of American Societies for Experimental Biology 2011;25:4253-63.
31. Naito Y, Williams-Fritze M, Duncan DR, et al. Characterization of the natural history of extracellular matrix production in tissue-engineered vascular grafts during neovessel formation. Cells, tissues, organs 2012;195:60-72.
32. Mirensky TL, Hibino N, Sawh-Martinez RF, et al. Tissue-engineered vascular grafts: does cell seeding matter? Journal of pediatric surgery 2010;45:1299-305.
33. Mirensky TL, Nelson GN, Brennan MP, et al. Tissue-engineered arterial grafts: long-term results after implantation in a small animal model. J Pediatr Surg 2009;44:1127-32; discussion 32-3.
34. Humphrey JD. Vascular adaptation and mechanical homeostasis at tissue, cellular, and sub-cellular levels. Cell biochemistry and biophysics 2008;50:53-78.
35. Greve JM, Les AS, Tang BT, et al. Allometric scaling of wall shear stress from mice to humans: quantification using cine phase-contrast MRI and computational fluid dynamics. American journal of physiology Heart and circulatory physiology 2006;291:H1700-8.
36. Delvoye P, Wiliquet P, Leveque JL, Nusgens BV, Lapiere CM. Measurement of mechanical forces generated by skin fibroblasts embedded in a three-dimensional collagen gel. The Journal of investigative dermatology 1991;97:898-902.
37. Bruno G, Todor R, Lewis I, Chyatte D. Vascular extracellular matrix remodeling in cerebral aneurysms. Journal of neurosurgery 1998;89:431-40.
38. Peters DG, Kassam AB, Feingold E, et al. Molecular anatomy of an intracranial aneurysm: coordinated expression of genes involved in wound healing and tissue remodeling. Stroke; a journal of cerebral circulation 2001;32:1036-42.
39. Kassam AB, Horowitz M, Chang YF, Peters D. Altered arterial homeostasis and cerebral aneurysms: a molecular epidemiology study. Neurosurgery 2004;54:1450-60; discussion 60-2.
40. Baek S, Rajagopal KR, Humphrey JD. A theoretical model of enlarging intracranial fusiform aneurysms. Journal of biomechanical engineering 2006;128:142-9.
41. Gleason RL, Humphrey JD. Effects of a sustained extension on arterial growth and remodeling: a theoretical study. Journal of biomechanics 2005;38:1255-61.
42. Gleason RL, Wilson E, Humphrey JD. Biaxial biomechanical adaptations of mouse carotid arteries cultured at altered axial extension. Journal of biomechanics 2007;40:766-76.
43. Naito Y, Lee YU, Yi T, et al. Beyond Burst Pressure: Initial Evaluation of the Natural History of the Biaxial Mechanical Properties of Tissue Engineered Vascular Grafts in the Venous Circulation Using a Murine Model. Tissue engineering Part A 2013.
44. Miller KS, Lee YU, Naito Y, Breuer CK, Humphrey JD. Computational model of the in vivo development of a tissue engineered vein from an implanted polymeric construct. Journal of biomechanics 2013.

45. Niklason LE, Yeh AT, Calle EA, Bai Y, Valentin A, Humphrey JD. Enabling tools for engineering collagenous tissues integrating bioreactors, intravital imaging, and biomechanical modeling. Proc Natl Acad Sci U S A 2010;107:3335-9.
46. Gleason RL, Gray SP, Wilson E, Humphrey JD. A multiaxial computer-controlled organ culture and biomechanical device for mouse carotid arteries. J Biomech Eng 2004;126:787-95.
47. Ferruzzi J, Bersi MR, Humphrey JD. Biomechanical Phenotyping of Central Arteries in Health and Disease: Advantages of and Methods for Murine Models. Annals of biomedical engineering 2013.
48. Collins MJ, Eberth JF, Wilson E, Humphrey JD. Acute mechanical effects of elastase on the infrarenal mouse aorta: implications for models of aneurysms. Journal of biomechanics 2012;45:660-5.
49. Ferruzzi J, Collins MJ, Yeh AT, Humphrey JD. Mechanical assessment of elastin integrity in fibrillin-1-deficient carotid arteries: implications for Marfan syndrome. Cardiovascular research 2011;92:287-95.
50. Wu W, Allen RA, Wang Y. Fast-degrading elastomer enables rapid remodeling of a cell-free synthetic graft into a neoartery. Nature medicine 2012;18:1148-53.
51. de Valence S, Tille JC, Mugnai D, et al. Long term performance of polycaprolactone vascular grafts in a rat abdominal aorta replacement model. Biomaterials 2012;33:38-47.
52. Kuwabara F, Narita Y, Yamawaki-Ogata A, et al. Novel small-caliber vascular grafts with trimeric Peptide for acceleration of endothelialization. The Annals of thoracic surgery 2012;93:156-63; discussion 63.
53. L'Heureux N, McAllister TN, de la Fuente LM. Tissue-engineered blood vessel for adult arterial revascularization. N Engl J Med 2007;357:1451-3.
54. McAllister TN, Maruszewski M, Garrido SA, et al. Effectiveness of haemodialysis access with an autologous tissue-engineered vascular graft: a multicentre cohort study. Lancet 2009;373:1440-6.
55. L'Heureux N, Dusserre N, Konig G, et al. Human tissue-engineered blood vessels for adult arterial revascularization. Nat Med 2006;12:361-5.
56. Wystrychowski W, McAllister TN, Zagalski K, Dusserre N, Cierpka L, L'Heureux N. First human use of an allogeneic tissue-engineered vascular graft for hemodialysis access. J Vasc Surg 2013.
57. Wagenseil JE, Mecham RP. Vascular extracellular matrix and arterial mechanics. Physiological reviews 2009;89:957-89.
58. Humphrey JD, Eberth JF, Dye WW, Gleason RL. Fundamental role of axial stress in compensatory adaptations by arteries. Journal of biomechanics 2009;42:1-8.
59. Stitzel JD, Pawlowski KJ, Wnek GE, Simpson DG, Bowlin GL. Arterial smooth muscle cell proliferation on a novel biomimicking, biodegradable vascular graft scaffold. Journal of biomaterials applications 2001;16:22-33.
60. Hasan A, Memic A, Annabi N, et al. Electrospun scaffolds for tissue engineering of vascular grafts. Acta biomaterialia 2013.
61. Wise SG, Byrom MJ, Waterhouse A, Bannon PG, Weiss AS, Ng MK. A multilayered synthetic human elastin/polycaprolactone hybrid vascular graft with tailored mechanical properties. Acta biomaterialia 2011;7:295-303.

62. Boland ED, Telemeco TA, Simpson DG, Wnek GE, Bowlin GL. Utilizing acid pretreatment and electrospinning to improve biocompatibility of poly(glycolic acid) for tissue engineering. Journal of biomedical materials research Part B, Applied biomaterials 2004;71:144-52.
63. Soletti L, Nieponice A, Hong Y, et al. In vivo performance of a phospholipid-coated bioerodable elastomeric graft for small-diameter vascular applications. Journal of biomedical materials research Part A 2011;96:436-48.
64. Nieponice A, Soletti L, Guan J, et al. In vivo assessment of a tissue-engineered vascular graft combining a biodegradable elastomeric scaffold and muscle-derived stem cells in a rat model. Tissue engineering Part A 2010;16:1215-23.
65. He W, Ma Z, Teo WE, et al. Tubular nanofiber scaffolds for tissue engineered small-diameter vascular grafts. Journal of biomedical materials research Part A 2009;90:205-16.